J. Fluid Mech. (2020), *vol*. 901, A23. © The Author(s), 2020.
Published by Cambridge University Press
doi:10.1017/jfm.2020.568

Extraction of the translational Eucken factor from light scattering by molecular gas

Lei Wu[1],†, **Qi Li**[1], **Haihu Liu**[2] **and Wim Ubachs**[3]

[1]Department of Mechanics and Aerospace Engineering, Southern University of Science and Technology, Shenzhen 518055, PR China

[2]School of Energy and Power Engineering, Xi'an Jiaotong University, Xi'an 710049, PR China

[3]Department of Physics and Astronomy, LaserLaB, Vrije Universiteit, De Boelelaan 1081, Amsterdam 1081 HV, The Netherlands

(Received 16 March 2020; revised 23 May 2020; accepted 6 July 2020)

Although the thermal conductivity of molecular gases can be measured straightforwardly and accurately, it is difficult to experimentally determine its separate contributions from the translational and internal motions of gas molecules. Yet, this information is critical in rarefied gas dynamics as the rarefaction effects corresponding to these motions are different. In this paper, we propose a novel methodology to extract the translational thermal conductivity (or equivalently, the translational Eucken factor) of molecular gases from the Rayleigh–Brillouin scattering (RBS) experimental data. From the numerical simulation of the Wu *et al.* (*J. Fluid Mech.*, vol. 763, 2015, pp. 24–50) model we find that, in the kinetic regime, in addition to bulk viscosity, the RBS spectrum is sensitive to the translational Eucken factor, even when the total thermal conductivity is fixed. Thus it is not only possible to extract the bulk viscosity, but also the translational Eucken factor of molecular gases from RBS light scattering spectra measurements. Such experiments bear the additional advantage that gas–surface interactions do not affect the measurements. By using the Wu *et al.* model, bulk viscosities (due to the rotational relaxation of gas molecules only) and translational Eucken factors of N_2, CO_2 and SF_6 are simultaneously extracted from RBS experiments.

Key words: rarefied gas flow

1. Introduction

The gas kinetic theory developed by Maxwell (1867) and Boltzmann (1872) has turned out to be extremely successful in describing the rarefied gas dynamics of dilute gas, and it has found a wide range of applications in space vehicle re-entry, microelectromechanical systems, shale gas transport and so on. Especially, when the intermolecular potentials are known, transport coefficients of monatomic gases such as the shear viscosity μ_s and thermal conductivity κ, obtained from the Chapman–Enskog expansion of the Boltzmann equation (Chapman & Cowling 1970) agree well with experimental data. However, when the Boltzmann equation was extended to the Wang-Chang & Uhlenbeck (1951) equation for molecular gases, difficulty arose in accurately determining the transport coefficients,

† Email address for correspondence: wul@sustech.edu.cn

e.g. the translational and internal Eucken factors (f_{tr} and f_{int}, respectively) that appear in the thermal conductivity of a molecular gas

$$\frac{\kappa M}{\mu_s} = \frac{3R}{2} f_{tr} + \left(c_v - \frac{3R}{2} \right) f_{int} \equiv c_v f_u, \tag{1.1}$$

where M is the molar mass, R is the universal gas constant, c_v is the molar heat capacity at constant volume and f_u is the total Eucken (1913) factor.

It is also difficult to determine f_{tr} and f_{int} experimentally, despite that the total thermal conductivity (or equivalently, the Eucken factor f_u) can be measured straightforwardly. However, in rarefied gas dynamics, f_{tr} is an important parameter since rarefaction effects corresponding to the translational and internal motions of gas molecules are generally different. For example, in thermal transpiration where the gas automatically moves from a cold region to a hot region in the absence of a pressure gradient (Maxwell 1879; Reynolds 1879), the mass flow rate is proportional to f_{tr}, rather than f_u (Porodnov, Kulev & Tuchvetov 1978; Loyalka & Storvick 1979; Loyalka, Storvick & Lo 1982). Although f_{tr} can be measured in thermal transpiration flows (Mason 1963; Gupta & Storvick 1970), the result cannot be accurate as it is hampered by the inaccurate gas–surface interaction (Sharipov 2011; Wu & Struchtrup 2017).

Recent advances in Rayleigh–Brillouin scattering (RBS) experiments of molecular gases provide an excellent method to retrieve the information on thermodynamic properties of gases (Pan, Shneider & Miles 2002, 2004; Meijer *et al.* 2010; Vieitez *et al.* 2010; Gerakis, Shneider & Barker 2013; Gu & Ubachs 2013; Gu *et al.* 2015), where the gas–surface interaction is absent, i.e. only a local volume inside the gas cell is probed by laser light, see figure 1. This extraction of gas information is achieved by comparing the experimental RBS line shapes with theoretical ones. The RBS line shape can be obtained by solving the linearized Boltzmann equation for monatomic gas and the Wang-Chang & Uhlenbeck (1951) equation for molecular gas (Sugawara, Yip & Sirovich 1968). However, due to the complexity of Boltzmann-type collision operators, simplified kinetic models like the Hanson & Morse (1967) model, on which the prevailing Tenti, Boley & Desai (1974) line shape models are based, were proposed. Most attention has been paid to the extraction of bulk viscosity, which is related only to the rotational relaxation time as the vibrational modes, even when they are activated fully or partially, remain 'frozen' at the high frequencies used in light scattering experiments (Meijer *et al.* 2010).

The Tenti model requires four input parameters: (i) the uniformity parameter y which is controlled by the shear viscosity, pressure, temperature, laser wavelength, and the angle of scattering; (ii) the internal degrees of freedom; (iii) the rotational relaxation time which determines the bulk viscosity in RBS experiments; and (iv) the effective thermal conductivity κ_e involved in the light scattering. Since the vibrational relaxation is 'frozen' in RBS experiments, the internal degrees of freedom only correspond to the rotational degrees of freedom. Similarly, in the determination of effective thermal conductivity κ_e the contribution from vibrational degrees of freedom should be subtracted (Wang *et al.* 2017, 2018; Wang, Ubachs & van de Water 2019),

$$\kappa_e = \frac{\mu_s}{M} \left(\frac{3R}{2} f_{tr} + \frac{d_r R}{2} f_{int} \right) \equiv \kappa - \frac{\mu_s d_v R}{2M} f_{int}, \tag{1.2}$$

where d_r is the number of rotational degrees of freedom and $d_v = 2c_v/R - 3 - d_r$ is the number of all other internal degrees of freedom that are able to hold heat energy. However, this subtraction imposes an uncertainty on the value of κ_e, because f_{int} and f_{tr} cannot

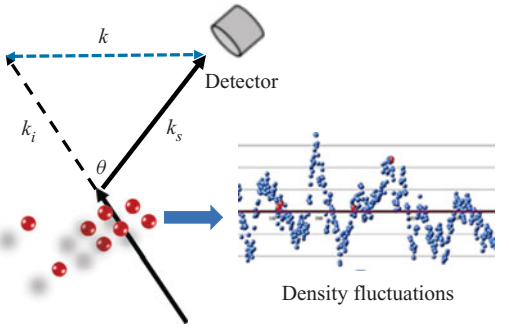

FIGURE 1. Schematic of the spontaneous RBS process, where the light is scattered by the spontaneous density fluctuations in the gas. The vectors k_i and k_s represent the incident and scattered light wave momentum vectors, respectively, while k represents the Brillouin scattering vector, in both directions for Stokes and anti-Stokes scattering. The scattering wavelength is $L = \pi/|\boldsymbol{k}_i| \sin(\theta/2)$. Figure modified from figure 1(*a*) in Wu & Gu (2020).

be determined accurately from previous theoretical and experimental works (Mason & Monchick 1962; Mason 1963; Gupta & Storvick 1970). Therefore, in order to extract the bulk viscosity accurately, the rotational relaxation time and translational Eucken factor should be varied simultaneously in gas kinetic models to find the minimum residual between the theoretical and experimental RBS line shapes. This cannot be achieved in the Tenti model, where f_{tr} is a function of the rotational relaxation time.

In this paper we will use the kinetic model proposed by Wu *et al.* (2015*b*), which not only allows an independent variation of bulk viscosity and translational Eucken factor, but also incorporates the physical velocity-dependent collision frequency of gas molecules, such that this kinetic model is reduced to the Boltzmann equation in the limit of infinite rotational relaxation time. We will show that the bulk viscosity and the translational Eucken factor can be extracted simultaneously from RBS experiments. Note that the prevailing direct simulation Monte Carlo (DSMC) method (Bird 1994) with the Borgnakke & Larsen (1975) phenomenological model is not used here, since it cannot always recover the bulk viscosity and thermal conductivity of molecular gas simultaneously, as we will show later.

2. Transport coefficients of molecular gas

The essential difference between monatomic and molecular gases is that molecules exhibit relaxation that exchanges translational and internal energies, which lead to several new transport coefficients including the bulk viscosity and internal thermal conductivity; they also affect the translational thermal conductivity, making f_{tr} less than 5/2 of monatomic gases (Mason & Monchick 1962).

For simplicity we consider the case where the rotational and vibrational internal modes are activated. In spatially homogeneous problems, the relaxation of rotational and vibrational temperatures (T_r and T_v, respectively) are described by the Jeans–Landau–Teller equation,

$$\frac{\partial T_\ell}{\partial t} = \frac{T_t - T_\ell}{\tau_\ell}, \quad \ell = r, v, \tag{2.1}$$

where τ_r and τ_v are, respectively, the rotational and vibrational relaxation times, and T_t is the translational temperature.

When the relaxation times are much smaller than the characteristic flow frequency ω (e.g. the sound frequency or the frequency associated with the scattering wave vector in RBS), i.e. $\omega\tau_\ell \ll 1$, the bulk viscosity can be exactly derived as follows (Chapman & Cowling 1970):

$$\mu_b = 2n_0 k_B T_t \frac{d_r\tau_r + d_v\tau_v}{(3+d_r+d_v)^2}, \tag{2.2}$$

where n_0 is the number density of the gas and k_B is the Boltzmann constant. However, when the characteristic flow frequency is comparable to or larger than τ_ℓ^{-1}, the bulk viscosity becomes frequency dependent (Bruno, Frezzotti & Ghiroldi 2015; Jaeger, Matar & Muller 2018; Wang *et al.* 2019); it can be roughly described by (Meador, Miner & Townsend 1996; Meijer *et al.* 2010)

$$\mu_b = 2n_0 k_B T_t \frac{\sum_\ell d_\ell\tau_\ell/(1+\omega^2\tau_\ell^2)}{\left[3+\sum_\ell d_\ell/(1+\omega^2\tau_\ell^2)\right]^2}. \tag{2.3}$$

At room temperature, τ_r is approximately 10^{-10} s, while τ_v is usually larger than 10^{-6} s. Since in RBS the light frequency is operated in the gigahertz domain, the relaxation of vibrational modes is 'frozen', so the measured bulk viscosity is only determined through

$$\frac{\mu_b}{\mu_s} = \frac{2d_rZ}{3(d_r+3)}, \quad Z = \frac{3\tau_r}{(d_r+3)\tau}, \tag{2.4a,b}$$

where Z is the rotational collision number, with $\tau = \mu_s/n_0k_BT_t$ being the mean collision time of gas molecules due to the translational motion.

Unlike the bulk viscosity (2.2) that can be exactly derived when $\omega\tau_\ell \ll 1$, the thermal conductivities of molecular gases can only be approximately determined from the Wang-Chang & Uhlenbeck (1951) equation through the Chapman–Enskog expansion (Chapman & Cowling 1970); the corresponding Eucken factors are (Mason & Monchick 1962)

$$\left.\begin{aligned} f_{tr} &= \frac{5}{2}\left[1 - \frac{5d_r}{4(d_r+3)Z}\left(1-\frac{2\rho D'}{5\mu_s}\right)\right], \\ f_{int} &= \frac{\rho D'}{\mu_s}\left[1 + \frac{15d_r}{4(d_r+d_v)(d_r+3)Z}\left(1-\frac{2\rho D'}{5\mu_s}\right)\right], \end{aligned}\right\} \tag{2.5}$$

where ρ is the mass density of the gas, D' is the average diffusion coefficient, which can be markedly different from the self-diffusion coefficient D if strong resonant collision occurs. The fact that f_{tr} decreases along with Z can be explained as follows: due to the internal energy exchanges, the translational thermal conductivity decreases because during the transport of gas molecules part of the translational energy is converted to the internal energy; the intensity of this conversion becomes stronger when Z decreases, and when D' increases. The internal Eucken factor f_{int} changes with respect to Z in opposite direction. This shows that (2.5) is physically reasonable.

It is clear from (2.5) that when the gas species is chosen, its dynamics is affected by two free parameters: the rotational collision number that determines the bulk viscosity and the average diffusion coefficient D' (or equivalently f_{tr}), which should guarantee the total thermal conductivity (as well as its components) to agree with experimental data. For monatomic gas, the structure of the Boltzmann collision operator ensures that f_{tr} is very close to 2.5, which agrees with experimentally measured values. Since it can be rigorously proved that the DSMC method and the Boltzmann equation are equivalent for

monatomic gas (Wagner 1992), DSMC can also produce reasonable values of thermal conductivity. However, despite the overwhelming success of DSMC over deterministic solvers of gas kinetic equations for hypersonic flow simulations, whether it can produce the exact translational and internal thermal conductivities of molecular gases or not has been overlooked. The variable-soft-sphere model has been developed to recover the experimental values of shear viscosity and self-diffusion coefficients, while the Borgnakke & Larsen (1975) phenomenological collision model has been developed to recover the energy exchange rate (Boyd 1990; Haas *et al.* 1994; Gimelshein, Gimelshein & Lavin 2002) so that the bulk viscosity is obtained exactly. However, whether the total thermal conductivities, f_{tr} and f_{int} have been accurately modelled in DSMC or not has not been investigated in detail (Gallis, Rader & Torczynski 2004) as, actually, there is no mechanism dedicated to recovering the thermal conductivity correctly. These parameters, however, affect the thermal transpiration (Gupta & Storvick 1970) and the RBS line shape (as we shall see in § 3.2 below).

The approximate solution (2.5) implies that the DSMC might also be able to recover the total thermal conductivity of molecular gas, by adjusting the self-diffusion coefficient. This is illustrated in figure 2, for the non-polar gas nitrogen and polar gas hydrogen chloride, where the self-diffusion coefficient D satisfies $\rho D/\mu_s = 1.34$ at room temperature. It can be seen that the thermal conductivities are functions of the diffusion coefficient D' and the inelastic collision probability Λ. Compared with (5.67) and (4.50) in the book by Bird (1994), Λ is related to the collision number Z through the Jeans equation (2.1) as

$$Z = \frac{1}{\Lambda}\frac{\alpha(5-2\omega)(7-2\omega)}{5(\alpha+1)(\alpha+2)}, \tag{2.6}$$

where α is the exponent in the variable-soft-sphere model and ω is the viscosity index such that the shear viscosity varies with the temperature as

$$\mu_s(T) = \mu_s(T_0)\left(\frac{T}{T_0}\right)^{\omega}. \tag{2.7}$$

Thus, if we know the total thermal conductivity and bulk viscosity of molecular gas from experiments, Z and Λ can be determined first, and then the average diffusion coefficient D' can be varied to recover the total thermal conductivity. Nevertheless, at the same values of bulk viscosity and thermal conductivity, the approximate solution (2.5) and DSMC with the phenomenological Borgnakke & Larsen (1975) model possess different values of f_{tr}, and one does not know which one is accurate, or maybe both are not. For hydrogen chloride, the resonant interaction leads to a significant reduction of $\rho D'/\mu_s$ from 1.34 to 0.89 (Mason & Monchick 1962); in order to recover the total thermal conductivity measured from experiments, figure 2(*b*) shows that the inelastic collision probability Λ in DSMC should approach unity, which seems not physical as the maximum possible rate of exchange between translational and internal energy is reached. If one wants to use a reasonable value of Λ (or the bulk viscosity), D' should be much smaller than the self-diffusion coefficient. This will pose another difficulty: in gas mixtures where both diffusion and thermal conductivity are important, how to recover them in DSMC with the Borgnakke & Larsen (1975) model? On the contrary, the approximate solution (2.5) seems to give a reasonable value of the inelastic collision probability.

Therefore, although the phenomenological Borgnakke & Larsen (1975) model has been widely used, we believe that more tests should be done to validate it. In addition, in terms of RBS application the DSMC is very time-consuming. This is because to compute a single

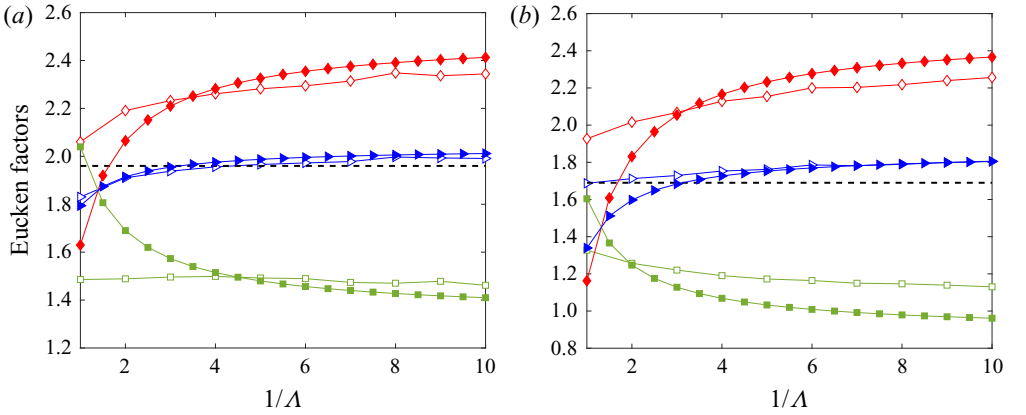

FIGURE 2. The thermal conductivity obtained from the analytical solution (2.5) and the DSMC at room temperature, as a function of the inelastic collision probability Λ. The open source DSMC code SPARTA (https://sparta.sandia.gov/) is used to simulate the Fourier flow between two parallel plates, at a Knudsen number of 0.05, and the translational and internal thermal conductivities are extracted in the bulk region (a few mean free paths away from the plates) using the Fourier heat conduction law. The variable-soft-sphere model is used and the self-diffusion coefficient D in DSMC takes the value of D'. Open diamonds, squares and triangles represent the translational, internal and total Eucken factors from (2.5), respectively, while the filled symbols are the corresponding results from DSMC. Dashed lines show the total Eucken factor obtained from experiments at a temperature of 300 K. (*a*) Nitrogen, $\rho D'/\mu_s = 1.34$; (*b*) hydrogen chloride, $\rho D'/\mu_s = 0.89$.

RBS line shape it would take several hours of wall-clock time (Bruno *et al.* 2006; Bruno, Frezzotti & Ghiroldi 2017), while to extract the bulk viscosity and translational Eucken factor (through the adjustment of average diffusion coefficient) from RBS experiments it needs hundreds of hours. Therefore, the Wu *et al.* (2015*b*) model will be used in this paper, since (i) it has the flexibility to adjust the bulk viscosity and translational Eucken factor independently; (ii) in the limit of no internal-translational energy exchange, the Boltzmann equation, DSMC and Wu *et al.* model all yield same results; and (iii) it can produce one RBS line shape in just a few seconds in a laptop, due to the fast spectral method for the Boltzmann collision operator (Wu *et al.* 2015*a*) and the general synthetic iterative scheme (Su *et al.* 2020).

3. The Wu *et al.* model for molecular gas

The spectrum of scattered light in spontaneous RBS processes shown in figure 1 is strongly influenced by the rarefaction parameter δ_{rp} (i.e. the ratio of the scattering wavelength L to the molecular mean free path)

$$\delta_{rp} = \frac{n_0 k_B T_0}{\mu_s(T_0) v_m} L \equiv 2\pi y, \tag{3.1}$$

where y is the uniformity parameter frequently used in RBS experiments, T_0 is the gas temperature,

$$v_m = \sqrt{\frac{2k_B T_0}{m}} \tag{3.2}$$

is the most probable speed and m is the mass of gas molecules.

The dynamics of molecular gas is described by Wang-Chang & Uhlenbeck (1951), where each individual energy level of molecules was assigned a velocity distribution function. This brings tremendous analytical and computational difficulties; therefore it is necessary to develop kinetic models to simplify the Boltzmann-type collision operator. In RBS, the Hanson & Morse (1967) model, on which the Tenti *et al.* (1974) model is based, serves this purpose. When the vibrational relaxation is 'frozen' in RBS experiments, the bulk viscosity in Tenti's model satisfies (2.4*a*,*b*). On the other hand, when the effective thermal conductivity κ_e in (1.2) and the bulk viscosity (controlled by Z) are known, the translational Eucken factor is uniquely determined as (Loyalka & Storvick 1979)

$$f_{tr} = \frac{5f_u^e + 10Z}{5 + 4Z}, \tag{3.3}$$

where $f_u^e = 2m\kappa_e/(3 + d_r)\mu_s k_B$.

However, since the interaction between molecules is not in all cases governed by a symmetric Maxwellian potential as assumed by Wang-Chang & Uhlenbeck (1951), (3.3) might not hold for all molecules. More seriously, in many previous papers f_u^e is chosen as f_u, such that the thermal conductivity due to the vibrational motion of gas molecules, which is not involved in RBS scattering, is considered. Therefore, a kinetic model for a molecular gas which allows the independent change of Z and f_{tr} is needed. The model developed by Wu *et al.* (2015*b*), which introduces two velocity distribution functions h_0 and h_2 to describe the system state, satisfies the following requirement:

$$\left.\begin{aligned}
&\frac{\partial h_0}{\partial t} + v_1\frac{\partial h_0}{\partial x_1} = \mathcal{C}_0 \equiv \mathcal{L}(h_0) - \nu_{eq}(\boldsymbol{v})h_0 \\
&\quad + \delta_{rp}\frac{f_{eq}}{Z}\left[(T - T_t)\left(v^2 - \frac{3}{2}\right) + \frac{4(\omega_0 - 1)}{15}q_t v_1\left(v^2 - \frac{5}{2}\right)\right], \\
&\frac{\partial h_2}{\partial t} + v_1\frac{\partial h_2}{\partial x_1} = \mathcal{C}_2 \equiv \delta_{rp}\left[\frac{d_r}{2}T_r f_{eq} - h_2\right] + \frac{d_r\delta_{rp}}{2Z}(T - T_r)f_{eq} \\
&\quad + \delta_{rp}\frac{2(Z + \omega_1 - 1)(1 - \delta)}{Z}q_r v_1 f_{eq},
\end{aligned}\right\} \tag{3.4}$$

where δ is the Schmidt number of the gas, $f_{eq}(\boldsymbol{v}) = \exp(-v^2)/\pi^{3/2}$ is the global equilibrium distribution function, $\mathcal{L}(h_0)$ is the gain part of the linearized Boltzmann collision operator $\mathcal{L}(h_0) = \int\!\!\int B[f_{eq}(\boldsymbol{v}')h_0(\boldsymbol{v}') + h_0(\boldsymbol{v}')f_{eq}(\boldsymbol{v}_*') - f_{eq}(\boldsymbol{v})h_0(\boldsymbol{v}_*)]\,\mathrm{d}\Omega\,\mathrm{d}\boldsymbol{v}_*$ and $\nu_{eq}(\boldsymbol{v}) = \int\!\!\int B f_{eq}(\boldsymbol{v}_*)\,\mathrm{d}\Omega\,\mathrm{d}\boldsymbol{v}_*$ is the equilibrium collision frequency, with $\boldsymbol{v}$ and $\boldsymbol{v}_*$ being the velocity of two molecules before the binary collision, $\boldsymbol{v}'$ and $\boldsymbol{v}_*'$ the corresponding velocities after collision, $\mathrm{d}\Omega$ the solid angle of binary scattering and B the elastic collision probability determined by the intermolecular potential. Here we consider the inverse power law intermolecular potential, where the shear viscosity is given by (2.7). For hard-sphere and Maxwellian molecules we have $\omega = 0.5$ and 1, respectively. The collisional behaviour of other gases usually falls between these two cases, and the viscosity index ω normally has value between 0.5 and 1 (Bird 1994). Details of the collision probability B have been presented by Wu *et al.* (2015*a*).

Note that in (3.4) the molecular velocity $\boldsymbol{v}$, spatial coordinate x_1 and time t have been normalized by the most probable speed v_m, the scattering wavelength L, and L/v_m, respectively. Also, the translational temperature is $T_t = \int (2v^2/3 - 1)h_0\,\mathrm{d}\boldsymbol{v}$, the rotational temperature is $T_r = (2/d_r)\int h_2\,\mathrm{d}\boldsymbol{v}$, the total temperature is $T = (3T_t + d_r T_r)/(3 + d_r)$,

the translational and rotational heat flux are, respectively, $q_t = \int (v^2 - 5/2)v_1 h_0 \, \mathrm{d}\boldsymbol{v}$ and $q_r = \int v_1 h_2 \, \mathrm{d}\boldsymbol{v}$.

While the bulk viscosity is determined by Z in (2.4*a*,*b*), the translational and internal Eucken factors,

$$f_{tr} = \frac{5}{2}\left(1 + \frac{1-\omega_0}{2Z}\right)^{-1}, \quad f_{int} = \delta^{-1}\left[1 + \frac{(1-\delta)(1-\omega_1)}{\delta Z}\right]^{-1}, \tag{3.5a,b}$$

are controlled by ω_0 and ω_1, respectively. This is one of the advantages of the Wu *et al.* model, where the two Eucken factors can be varied independently, while in the Tenti model f_{tr} is uniquely determined by Z in (3.3).

The RBS spectrum $S = \int \mathrm{Re}(\hat{h}_0) \, \mathrm{d}\boldsymbol{v}$ of a molecular gas, where Re is the real part of a variable, can be obtained by solving the following equations iteratively (Wu *et al.* 2015*b*):

$$\hat{h}_0^{(j+1)}(\boldsymbol{v}) = \frac{f_{eq} + \hat{\mathcal{C}}_0^{(j)} + \nu\hat{h}_0^{(j)}}{2\pi i(f_s - v_1) + \bar{\nu}}, \quad \hat{h}_2^{(j+1)}(\boldsymbol{v}) = \frac{\hat{\mathcal{C}}_2^{(j)} + \nu\hat{h}_2^{(j)}}{2\pi i(f_s - v_1) + \bar{\nu}}, \tag{3.6a,b}$$

where j is the iteration step, f_s is the frequency shift in the scattering process normalized by v_m/L, and $\bar{\nu} = 1.5\delta_{rp}(1 + 1/Z)$ is chosen to ensure the stability of iterations. Given the uniformity y and frequency shift f_s, the iteration is terminated when the relative difference in the RBS spectrum between two consecutive iterations is less than 10^{-6}. Starting from zero disturbance (i.e. $\hat{h}^{(0)} = \hat{h}^{(2)} = 0$), typically 20 iterations are sufficient to reach convergence at any value of y when the general synthetic iterative scheme (Su *et al.* 2020) is used; and only a few seconds is needed to compute a line shape on a laptop.

3.1. *Role of the rotational collision number*

When y is small, the gas dynamics is described by the collisionless Boltzmann equation so any internal relaxations are frozen. That is, the RBS spectrum adopts a Gaussian shape determined solely by the temperature. To study the influence of the rotational collision number on the RBS line shapes we need to choose larger values of y.

Figure 3 shows the RBS spectra for $y = 4$. It can be seen that the spectrum near the central Rayleigh peak increases with Z. Also, for diatomic gases ($d_r = 2$), the position of the side Brillouin peak shifts from $f_s = 0.83$ to 0.90 when Z increases from 2 to 100, while in the case of nonlinear polyatomic gases ($d_r = 3$) this peak moves from 0.81 to 0.90. Since this position is approximately determined by the sound speed normalized by the most probable speed v_m, it is concluded that the rotational relaxation is gradually frozen with increasing Z, such that the sound speed of the molecular gas increases from $\sqrt{(5 + d_r)/2(3 + d_r)}$ to that of a monatomic gas $\sqrt{5/6}$. Note that the collision number corresponding to vibrational modes is of the order of 10^4 for CO_2 and SF_6, and even larger for other molecules (Meijer *et al.* 2010). Therefore, this example further confirms that, when applying the gas kinetic model, the internal degrees of freedom should be the rotational degrees of freedom d_r, and the total thermal conductivity should only take into account the contribution from the translational and rotational motions. Indeed, in the analysis of experimental RBS spectra it was concluded that the vibrational relaxation was found to be frozen in various molecular gases (Wang *et al.* 2017, 2018, 2019).

3.2. *Role of the translational Eucken factor*

In the hydrodynamic regime (i.e. when y is large), the RBS line shape is determined by the total thermal conductivity, while in the free-molecular regime only the gas temperature

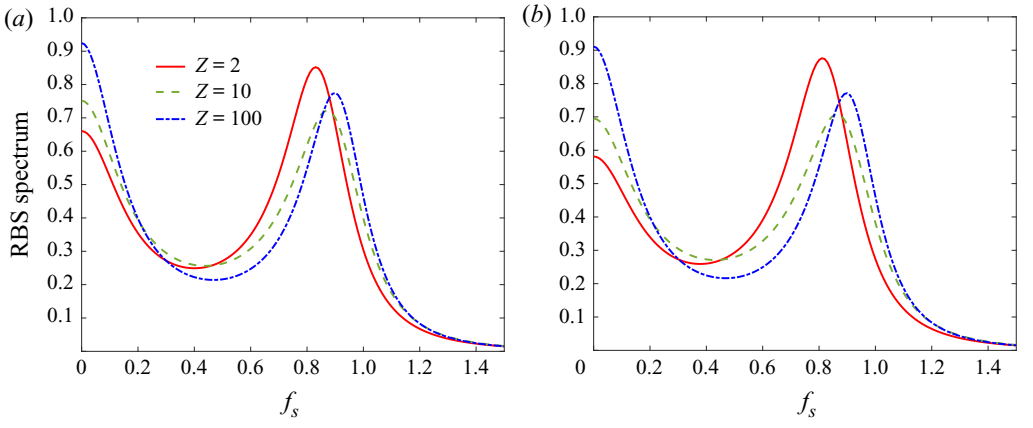

FIGURE 3. Computed RBS spectra showing the influence of rotational collision number in (*a*) a diatomic gas and (*b*) nonlinear polyatomic gas with $d_r = 3$, when $f_{tr} = f_{int} = 2$ and $y = 4$. In this and following figures, if not further specified, the RBS spectrum is normalized by the area $\int_{-\infty}^{\infty} S(f_s)\,\mathrm{d}f_s$ of each line shape.

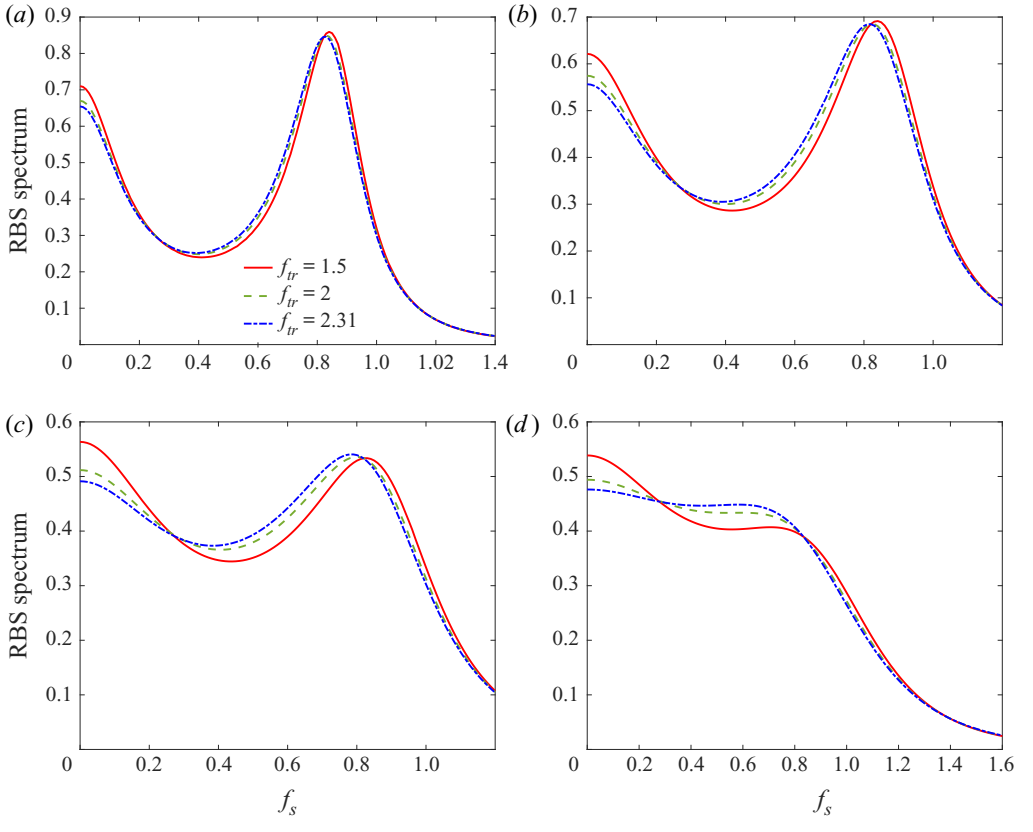

FIGURE 4. Computed RBS spectra displaying the influence of translational Eucken factor on RBS spectra of molecular gases with $d_r = 2$ and $d_v = 0$, when the total Eucken factor is $f_u = 2$ and the rotational collision number is $Z = 2$. (*a*) $y = 4$; (*b*) $y = 3$; (*c*) $y = 2$; (*d*) $y = 1$.

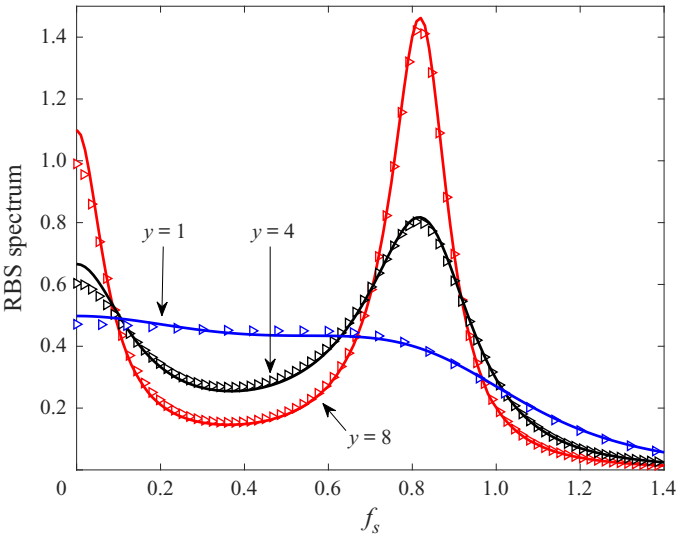

FIGURE 5. Computed RBS spectra showing the influence of f_{tr} on the RBS spectra of Maxwellian molecules with $d_r = 3$ and $d_v = 15$. The rotational collision number is $Z = 3$ and the total Eucken factor is $f_u = 1.429$. Triangles, $f_{tr} = 2.5$; lines, $f_{tr} = 2$.

determines the Gaussian line shape. However, the role of thermal conductivity in the kinetic regime, as an intermediate between these two limiting cases, is not *a priori* determined. Here we investigate the influence of f_{tr} on the RBS line shape when the total thermal conductivity (or equivalently f_u) is fixed. In this case, the internal Eucken factor can be calculated as $f_{int} = [(3 + d_r + d_v)f_u - 3f_{tr}]/(d_r + d_v)$.

We first consider the case where the vibrational degrees of freedom are not activated, i.e. $d_v = 0$; this occurs in, for example, oxygen at a temperature (e.g. room temperature) far smaller than the characteristic temperature of activation (around 2274 K) of the vibrational energy. We choose the total Eucken factor $f_u = 2$ and the rotational collision number $Z = 2$. The computational results for the kinetic regime are summarized in figure 4, where we see that the variation of f_{tr} leads to a strong change of the RBS line shape: the RBS spectrum near the Rayleigh peak decreases when f_{tr} increases; the strongest variation occurs around $y \sim 1$, and vanishes when $y \gtrsim 5$ or $y \lesssim 0.2$, i.e. in the hydrodynamic regime and in the near-collisionless regime, respectively.

We then consider the case when the vibrational degrees of freedom are activated. For example, $d_r = 3$ and $d_v = 15$ for SF_6 at room temperature. In this case, even at relatively large values of y, different values of f_{tr} lead to different RBS spectra (the difference is most prominent at the relative intensity of the central Rayleigh peak), see figure 5. This is because only the translational and rotational heat conductivities are reflected in RBS spectra (Wang *et al.* 2017, 2018, 2019), and their sum varies with f_{tr} even when f_u is fixed.

4. Extraction of bulk viscosity and translational Eucken factor

From the above numerical simulations we see that the RBS line shape is affected by Z and f_{tr}. Here we compare the theoretical RBS line shapes based on the Wu *et al.* model with experimental ones, to extract both bulk viscosity and translational Eucken factor.

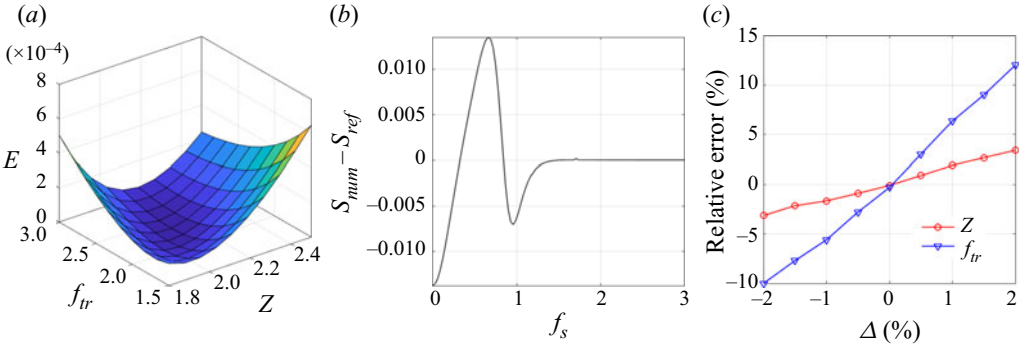

FIGURE 6. (*a*) The error function (4.1) when the relative error in pressure is $\Delta = 2\,\%$. (*b*) The difference in numerical (when E is minimum) and reference spectra when $\Delta = 2\,\%$. (*c*) Relative errors in the extracted Z and f_{tr}.

4.1. *An analysis of uncertainties in extracting Z and f_{tr}*

Uncertainties in pressure, temperature, wavelength, scattering angle and full width at half-maxima (FWHM) of the instrumental resolution are inevitable in RBS experiments, which affect the accuracy in extracting Z and f_{tr}. Here, uncertainties will be quantified in an error modelling approach. To be specific, we first generate the reference spectrum S_{ref} using the Wu *et al.* model with designated values of Z, f_{tr}, f_{int} and the instrumental function. Then we assume one of the measured parameters has an uncertainty while others are accurate. Many numerical spectra S_{num} will be generated with different values of Z and f_{tr}, but the same value of total Eucken factor f_u; this corresponds to the case that the total thermal conductivity is known but its separate contributions from the translational and internal motions of gas molecules are not known. Then the 'real' values of Z and f_{tr} are extracted when the following error:

$$E(Z, f_{tr}) = \int_0^\infty (S_{ref} - S_{num})^2 \, \mathrm{d}f_s, \tag{4.1}$$

reaches the minimum value. Without loss of generality we consider the Maxwell gas with $d_r = 2$, $d_v = 0$ and $Z = f_{tr} = f_{int} = y_{ref} = 2$ in the reference solution.

First, suppose the 'real' number density of gas molecules is larger than the average number density n_0 by $n_0\Delta$ per cent. According to (3.1), the y parameter used in the 'numerical' spectra is $y_{num} = y_{ref}(1 + \Delta)$. Given the value of Δ, we obtain the error function $E(Z, f_{tr})$, which possesses a global minimum in the $Z - f_{tr}$ space, see figure 6(*a*). Thus Z and f_{tr} can be extracted from this minimum point through cubic interpolation, these are shown in figure 6(*c*). It is seen that (i) the uncertainties in Z and f_{tr} are nearly linear functions of Δ; and (ii) a 1 % uncertainty in the gas pressure yields approximately 2 % and 6 % uncertainties in Z and f_{tr}, respectively. The absolute difference between the numerical and reference spectra is shown in figure 6(*b*), where we see large discrepancies occur around the Rayleigh and Brillouin peaks.

Second, the influence of the relative errors Δ_T and Δ_θ in temperature and scattering angle on the extracted Z and f_{tr} is shown in figure 7(*d*,*e*), from which we see that Z can be extracted with fair accuracy, while the error in f_{tr} is large. However, the influence of the scattering angle is larger, especially when the 'real' scattering angle is less than the measured one. The absolute difference between the numerical and reference spectra

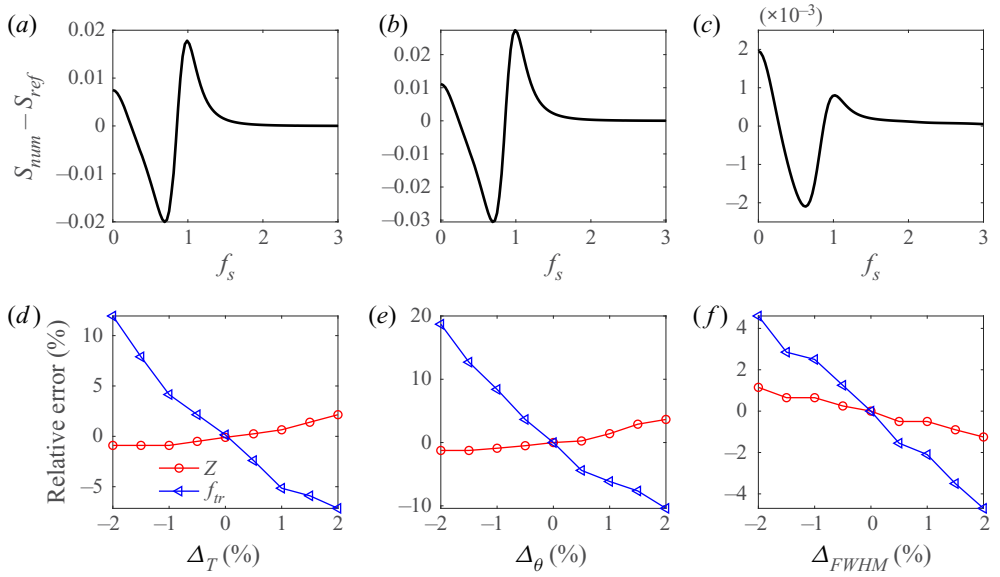

FIGURE 7. Effect of the relative error in (*a*,*d*) temperature, (*b*,*e*) scattering angle and (*c*,*f*) FWHM. (*a–c*) The difference in numerical (when E in (4.1) is minimum) and reference spectra when $\Delta = 2\,\%$. (*d–f*) Relative errors in the extracted Z and f_{tr}. The reference scattering angle is 90° as used in most RBS experiments.

is shown in figure 7(*a*,*b*), where we see that, unlike the case of uncertainty in number density, the discrepancy around the Brillouin peak is larger than that around the Rayleigh peak.

Third, the effect of the uncertainty Δ_λ in wavelength is the same as that caused by a $-4\Delta_\lambda/\pi$ uncertainty in scattering angle when the scattering angle is 90°. Fourth, we consider the influence of FWHM in the following instrumental function:

$$I = \left\{1 + \left(\frac{2 \cdot \mathrm{FSR}}{\pi \cdot \mathrm{FWHM}}\right)^2 \sin^2\left(\frac{\pi}{\mathrm{FSR}} f_s\right)\right\}^{-1}, \tag{4.2}$$

where we take FWHM = 0.15 and free spectral range FSR = 5 as relevant in the RBS experiment (Gu & Ubachs 2013). Results in figures 7(*c*) and 7(*f*) show that uncertainties in Z and f_{tr} are approximately one, and twice of that in FWHM.

Finally, in addition to these systematic errors, there is still noise in the spectrum. However, the advanced scattering set-up involving the combination of a powerful narrowband laser with an enhancement cavity as well as signal averaging over several hours yields high signal-to-noise spectral profiles with uncertainty below the 1 % level (Gu *et al.* 2012). Thus its influence on the extraction of Z and f_{tr} is negligible.

In recent RBS experiments (Wang *et al.* 2017, 2018, 2019), the uncertainties in number density, temperature, scattering angle and wavelength are approximately 0.25 %, 0.03 %, 0.3 % and 0.25 %, respectively. Therefore, the induced uncertainty in Z and f_{tr} is less than 2 %. However, the uncertainty in FWHM can be as high as 3 % (Wang *et al.* 2017), which results in 3 % and 6 % uncertainties in Z and f_{tr}, respectively. By using more accurate devices the uncertainty in FWHM may be reduced (Shang *et al.* 2019).

Case	T (K)	$10^5\mu_s$	100κ	P (bar)	y	ω	μ_b/μ_s	f_{tr}	f_{int}	f'_{tr}	f'_{int}	f''_{tr}	f''_{int}
(a)	254.7	1.57	2.28	2.563	1.73	0.80	0.48	2.16	1.65	2.17	1.58	2.12	1.61
(b)	275.2	1.67	2.44	2.784	1.70	0.78	0.61	2.25	1.53	2.24	1.52	2.14	1.59
(c)	296.7	1.77	2.60	3.000	1.66	0.76	0.69	2.31	1.47	2.27	1.50	2.16	1.58
(d)	336.6	1.95	2.88	3.400	1.61	0.74	0.94	2.43	1.33	2.33	1.45	2.18	1.56

TABLE 1. Experimental conditions in RBS of N_2 (Gu & Ubachs 2013) and extracted values of the bulk viscosity and translational/internal Eucken factor based on the Wu *et al.* model (3.4). The shear viscosity μ_s and total thermal conductivity κ are shown in SI units. The translational and internal Eucken factors f'_{tr} and f'_{int} are calculated according to (2.5) with $\rho D'/\mu_s = 1.32$ (Mason & Monchick 1962), using the extracted rotational collision number related to the bulk viscosity (2.4*a*,*b*), while f''_{tr} and f''_{int} are also calculated according to (2.5) using the rotational collision number from Parker (1959).

4.2. N_2

We first extract the bulk viscosity and translational Eucken factor of N_2 based on the experimental data of Gu & Ubachs (2013), where the laser wavelength of 366.8 nm is used and the scattering angle is 90°, i.e. $\theta = \pi/2$. Therefore, the effective wavelength is $L = 259.4$ nm. The rotational and vibrational degrees of freedom of N_2 in the experimental condition are $d_r = 2$ and $d_v = 0$, respectively. The shear viscosity and thermal conductivity are calculated based on the Sutherland formula (White 1998). The viscosity index ω is calculated according to (2.7) based on the Sutherland formula and listed in table 1. The translational and internal Eucken factors in the Wu *et al.* model (3.4) are chosen to recover the correct value of the thermal conductivity.

From the above results we find that the error function $E(Z, f_{tr})$ has one global minimum and is convex. Therefore, to accurately and efficiently determine Z and f_{tr}, we adopt the following procedure.

(i) We fix the value of f_{tr}, vary the value of Z, and calculate the RBS spectrum based on the Wu *et al.* model. Then the obtained analytical spectrum is convolved with the instrumental response function to yield the spectrum $S_{WU}(f_s)$. The error is defined as

$$E(Z) = \sum_{\ell=1}^{N} \frac{\{S_{exp}[f_s(\ell)] - S_{WU}[f_s(\ell)]\}^2}{N}, \tag{4.3}$$

where N is the number of discrete frequencies measured in experiments. The minimum error $E_m(f_{tr})$ is found by fitting E as the quartic polynomial function of Z and finding the minimum of this quartic function. Typically six different values of Z are calculated.

(ii) Repeat (i) for different values of f_{tr}. Typically six different values of f_{tr} are calculated.

(iii) Fitting $E_m(f_{tr})$ as the quartic polynomial function of f_{tr} we can determine f_{tr} corresponding to the minimum point of this quartic function.

(iv) With f_{tr} determined in (iii) we do (i) once again to determine Z. Hence the bulk viscosity is obtained according to (2.4*a*,*b*).

Comparisons between the experimental data and the theory (3.4) are visualized in figure 8. The residuals between the experimental and theoretical line shapes are generally within 1 %. According to the acoustic experiment (Lambert 1977) the rotational relaxation

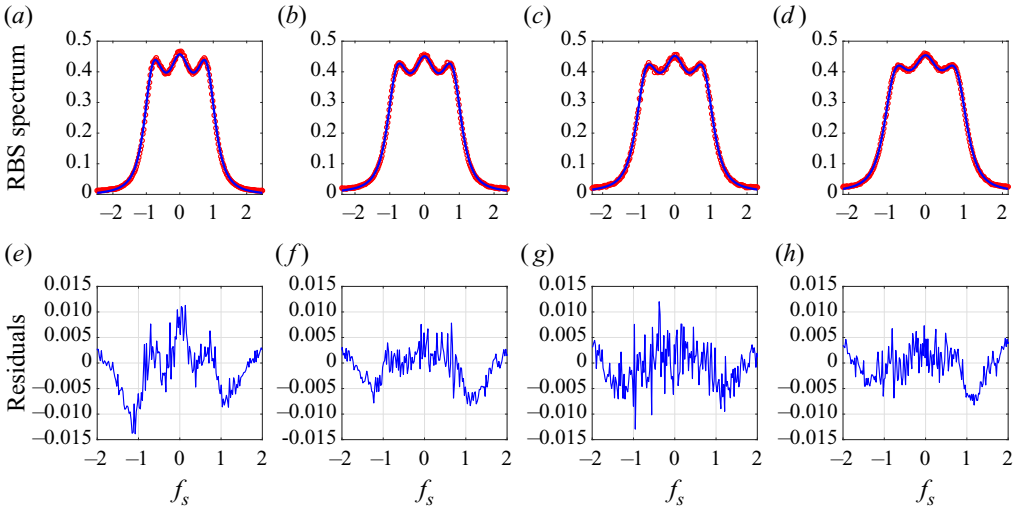

FIGURE 8. Extraction of the bulk viscosity and translational Eucken factor of N_2 from the experimental RBS spectra S_{exp} (circles) measured by Gu & Ubachs (2013). Lines in panels (*a–d*) show the RBS spectra S_{WU} obtained from the Wu *et al.* model with the minimum error (4.3) over a wide range of f_{tr} and Z, while those in panels (*e–h*) show the corresponding residuals between the experimental and theoretical spectra. Experimental conditions and extracted parameters are summarized in table 1.

time of N_2 at standard temperature and pressure is $\tau_r = 7.4 \times 10^{-10}$ s, therefore according to (2.4*a*,*b*) the bulk viscosity is $\mu_b = 2p\tau_r d_r/(3 + d_r)^2 = 1.18 \times 10^{-5}$ kg m^{-1} s^{-1}, which agrees well with the extracted bulk viscosity $\mu_b = 1.22 \times 10^{-5}$ kg m^{-1} s^{-1} at $T =$ 296.7 K.

The translational and internal Eucken factors are also extracted from the RBS experiment. We would like to compare these values with analytical solutions (2.5) derived by Mason & Monchick (1962) from the Wang-Chang & Uhlenbeck (1951) equation. In the paper of Mason & Monchick (1962), $\rho D'/\mu$ takes the value of 1.32 for nitrogen, for the temperatures listed in table 1. With the extracted rotational collision number Z from the RBS experiment, we can assess the accuracy of analytical expressions for translational and internal Eucken factors. Results are compared with the corresponding extracted values in table 1. The agreements between f_{tr} and f'_{tr} as well as f_{int} and f'_{int} are good, with maximum relative deviation less than 10 %. We also calculate the analytical translational Eucken factors f''_{tr} and f''_{int} by using the rotational collision number from the theory of Parker (1959), and find larger deviations from the experimentally extracted values. Generally speaking, compared with the transport coefficients obtained from the Boltzmann equation for monatomic gas, where the relative deviation is less than ∼2 %, analytical transport coefficients of molecular gas (2.5) give less satisfactory agreements with the experimental data, probably due to the introduced approximations in analytical derivations.

4.3. CO_2

We now extract the bulk viscosity and translational Eucken factor of CO_2 based on the experimental data of Gu *et al.* (2014) at the temperature of 296.5 K. The laser wavelength is 366.8 nm and the scattering angle is 90°, thus the effective scattering wavelength is $L = 259.4$ nm. The shear viscosity is $\mu_s = 1.49 \times 10^{-5}$ kg m^{-1} s^{-1} and the thermal

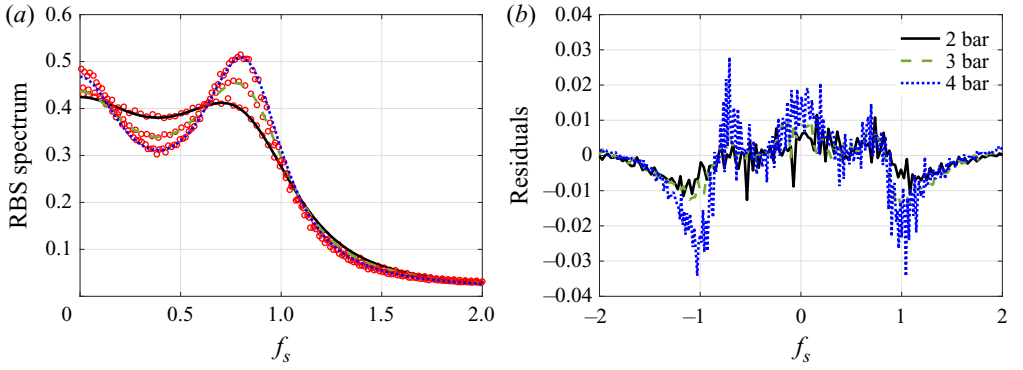

FIGURE 9. Same as figure 8, except the experimental data of CO_2 measured by Gu, Ubachs & van de Water (2014) is used here. The y parameters corresponding to the pressures 2, 3 and 4 bar are $y = 1.66$, 2.48 and 3.31, respectively.

conductivity is $\kappa = 1.67 \times 10^{-2}$ W K^{-1} m^{-1}. The viscosity index used in the Boltzmann equation is $\omega = 0.933$ (Chapman & Cowling 1970), the rotational degrees of freedom is $d_r = 2$ and the vibrational degrees of freedom is $d_v = 1.87$, using the data from the National Institute of Standards and Technology. Comparisons between the experimental and theoretical RBS line shapes are shown in figure 9, where the extracted rotational collision numbers are $Z = 1.72$, 1.56, 1.64, the translational Eucken factors are $f_{tr} = 2.30$, 2.23 and 2.18, and the internal Eucken factors are $f_{int} = 1.28$, 1.34 and 1.37, at pressures 2, 3 and 4 bar, respectively. We do not consider the case of 1 bar pressure because the uniformity parameter is $y = 0.83$ so that the line shape is not sensitive to f_{tr} and Z. Taking the average value we find that the translational and internal Eucken factors are $f_{tr} = 2.24$ and $f_{int} = 1.33$, respectively. The average value for the rotational collision number is $Z = 1.60$ and hence the bulk viscosity is $\mu_b = 6.6 \times 10^{-6}$ kg m^{-1} s^{-1}. Note that the rotational relaxation time of CO_2 at standard temperature and pressure is $\tau_r = 3.8 \times 10^{-10}$ s (Lambert 1977), therefore the bulk viscosity is $\mu_b = 6.1 \times 10^{-6}$ kg m^{-1} s^{-1}, which agrees well with the bulk viscosity extracted from the RBS experiment (Gu *et al.* 2014) using the Wu *et al.* model (3.4). Note that this bulk viscosity only takes into account the contribution from rotational relaxation; it is smaller than that obtained from the acoustic experiment by approximately four orders of magnitude (Lambert 1977; Pan, Shneider & Miles 2005).

4.4. SF_6

The experimental data of Wang *et al.* (2017) for SF_6 molecules recorded at pressures 0.754, 1.002, 2.002, 3, 4 and 5 bar are compared with the Wu *et al.* model, where the laser wavelength is 403 nm and the scattering angle is 89.6°, so the effective wavelength is $L = 286$ nm. With the viscosity data given by Quinones-Cisneros, Huber & Deiters (2012) we find that the shear viscosity is $\mu_s = 1.52 \times 10^{-5}$ kg m^{-1} s^{-1} and the viscosity index is $\omega = 0.885$ at temperature 298 K, while the heat conductivity is $\kappa = 1.30 \times 10^{-2}$ W m^{-1} K^{-1}. The rotational degrees of freedom is $d_r = 3$, while from the heat capacity data of Guder & Wagner (2009) we have $d_v = 15.32$. Comparisons between the experimental and theoretical RBS line shapes are shown in figure 10, where the extracted rotational collision numbers are $Z = 1.85$, 1.81, 1.90, 2.25, 2.64 and 3.31, while the translational Eucken factors are $f_{tr} = 2.29$, 2.23, 2.10, 2.07, 1.80 and 2.07, at

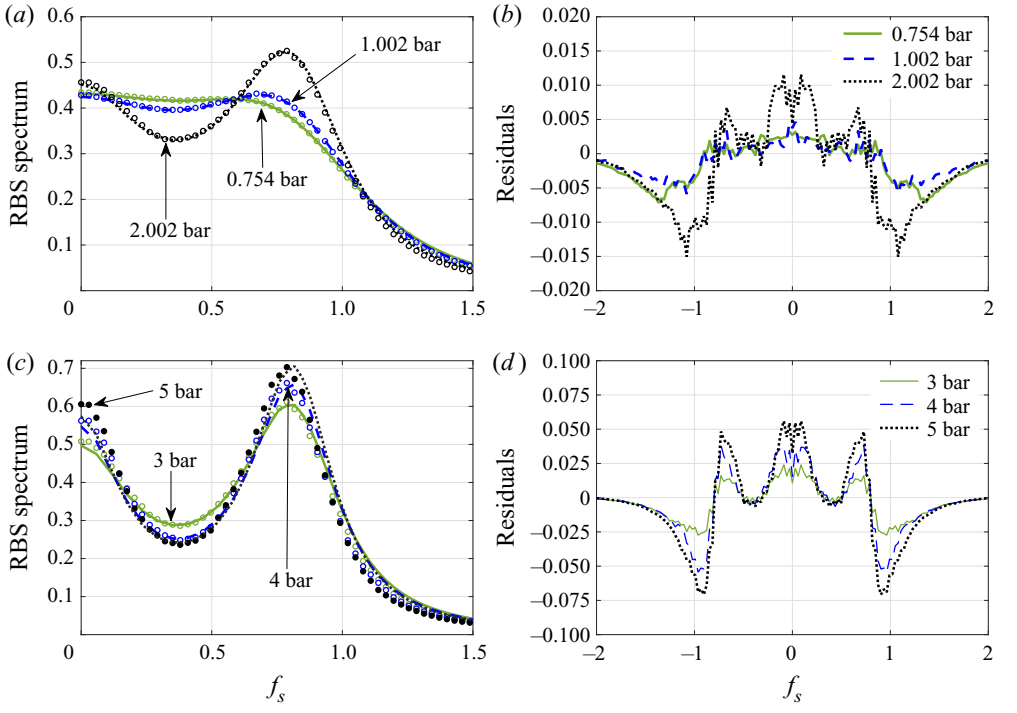

FIGURE 10. Same as figure 9, except the experimental data of SF_6 measured by Wang *et al.* (2017) is used here. The y parameters corresponding to the pressures 0.754, 1.002, 2.002, 3, 4 and 5 bar are $y = 1.22$, 1.64, 3.26, 4.88, 6.49 and 8.14, respectively.

pressures 0.754, 1.002, 2.002, 3, 4 and 5 bar, respectively. It is noted from figure 10(*c*,*d*) that the residuals between experimental and theoretical data increase significantly with pressure; it is postulated by Wang *et al.* (2017) that this might be due to the dense gas effect. However, the simulation results based on the Enskog–Vlasov equation, which takes into account the dense gas effect, still produce line shapes that have large deviations from the RBS experimental data, see figure 8 in Bruno & Frezzotti (2019). We leave this to future investigation and in the present paper we consider the extracted gas thermodynamic properties for pressure below 3 bar. Taking the average value at pressures of 0.754, 1.002 and 2.002 bars we have $f_{tr} = 2.21$ and $f_{int} = 1.28$. The average value for Z is 1.85, hence the ratio of bulk to shear viscosities is 0.62. Note that the rotational relaxation time of SF_6 at standard temperature and pressure is $\tau_r = 6 \times 10^{-10}$ s (Haebel 1968), therefore the viscosity ratio is $\mu_b/\mu_s = 0.66$, which agrees with the extracted value from the RBS experiment. Note that again this bulk viscosity only takes into account the contribution from the rotational relaxation of gas molecules.

5. Conclusions

We have analysed how an RBS spectrum in the kinetic regime (when the uniformity parameter falls in the region $1.2 \lessapprox y \lessapprox 3.3$) is sensitive to both the bulk viscosity and the translational Eucken factor f_{tr} and how the effect of these thermodynamic gas properties can be disentangled and determined separately from experiments. This is because for the very small values of y, collisions are virtually absent and the RBS spectrum approaches

that of a Gaussian (determined by temperature only), while for the very large values of y, the hydrodynamic regime is entered where only the total thermal conductivity is important. The Wu *et al.* (2015*b*) model is used to extract the bulk viscosity (due to the rotational relaxation of gas molecules only) and f_{tr} from recent RBS experiments of N_2, CO_2 and SF_6. The extracted bulk viscosity agrees well with the measurements from acoustic experiments when only the rotational relaxation is considered. For the extraction of f_{tr}, our method using the RBS line shapes is unique. This is because historically f_{tr} is measured in thermal transpiration flows in the kinetic regime, but this measurement approach is essentially hampered by gas–surface boundary effects; this problem is entirely absent in RBS experiments, since only a local volume inside the gas cell is probed by the laser light.

Although the extracted value of f_{tr} has no application in hydrodynamic flows where only the total thermal conductivity is important, it will affect the heat transfer and flow patterns in rarefied gas flows, as the rarefaction effects corresponding to the translational and internal motions are different due to the difference between the mean molecular collision time and the rotational/vibrational relaxation time. Thus, when analysing the results of RBS spectral measurements in the context of presented theoretical approach, the RBS experiments provide critical information on translational/internal Eucken factors. This will allow for more reliable simulations of rarefied gas dynamics.

Acknowledgements

This work is supported by the National Natural Science Foundation of China (No. 51876170), the Natural Science Basic Research Plan in Shaanxi Province of China (No. 2019JM-343) and the National Key Research and Development Project of China (No. 2016YFB0200902).

Declaration of interests

The authors report no conflict of interest.

REFERENCES

BIRD, G. A. 1994 *Molecular Gas Dynamics and the Direct Simulation of Gas Flows*. Oxford University Press.

BOLTZMANN, L. 1872 Weitere Studien über das Wärmegleichgewicht unter Gasmolekülen. *Sitz.ber. Akad. Wiss. Wien* **66**, 275–370.

BORGNAKKE, C. & LARSEN, P. S. 1975 Statistical collision model for Monte Carlo simulation of polyatomic gas mixture. *J. Comput. Phys.* **18** (4), 405–420.

BOYD, I. D. 1990 Rotational-translational energy transfer in rarefied nonequilibrium flows. *Phys. Fluids* A **2**, 447–452.

BRUNO, D., CAPITELLI, M., LONGO, S. & MINELLI, P. 2006 Monte Carlo simulation of light scattering spectra in atomic gases. *Chem. Phys. Lett.* **422**, 571–574.

BRUNO, D. & FREZZOTTI, A. 2019 Dense gas effects in the Rayleigh–Brillouin scattering spectra of SF6. *Chem. Phys. Lett.* **731**, 136595.

BRUNO, D., FREZZOTTI, A. & GHIROLDI, G. P. 2015 Oxygen transport properties estimation by classical trajectory–direct simulation Monte Carlo. *Phys. Fluids* **27**, 057101.

BRUNO, D., FREZZOTTI, A. & GHIROLDI, G. P. 2017 Rayleigh–Brillouin scattering in molecular oxygen by CT–DSMC simulations. *Eur. J. Mech. B/Fluids* **64**, 8–16.

CHAPMAN, S. & COWLING, T. G. 1970 *The Mathematical Theory of Non-uniform Gases*. Cambridge University Press.

EUCKEN, A. 1913 Über das Wärmeleitvermögen, die spezifische Wärme und die innere Reibung der Gase. *Phys.* Z **14**, 324.

GALLIS, M. A., RADER, D. J. & TORCZYNSKI, J. R. 2004 A generalized approximation for the thermophoretic force on a free-molecular particle. *Aerosol Sci. Technol.* **38**, 692–706.

GERAKIS, A., SHNEIDER, M. N. & BARKER, P. F. 2013 Single-shot coherent Rayleigh–Brillouin scattering using a chirped optical lattice. *Opt. Lett.* **38** (21), 4449.

GIMELSHEIN, N. E., GIMELSHEIN, S. F. & LAVIN, D. A. 2002 Vibrational relaxation rates in the direct simulation Monte Carlo method. *Phys. Fluids* **14**, 4452.

GU, Z. & UBACHS, W. 2013 Temperature-dependent bulk viscosity of nitrogen gas determined from spontaneous Rayleigh–Brillouin scattering. *Opt. Lett.* **38** (7), 1110.

GU, Z., UBACHS, W., MARQUES, W. & VAN DE WATER, W. 2015 Rayleigh–Brillouin scattering in binary-gas mixtures. *Phys. Rev. Lett.* **114**, 243902.

GU, Z., UBACHS, W. & VAN DE WATER, W. 2014 Rayleigh–Brillouin scattering of carbon dioxide. *Opt. Lett.* **39**, 3301.

GU, Z., VIEITEZ, M. O., VAN DUIJN, E. J. & UBACHS, W. 2012 A Rayleigh–Brillouin scattering spectrometer for ultraviolet wavelengths. *Rev. Sci. Instrum.* **83**, 053112.

GUDER, C. & WAGNER, W. 2009 A reference equation of state for the thermodynamic properties of sulfur hexafluoride (SF6) for temperatures from the melting line to 625 K and pressures up to 150 MPa. *J. Phys. Chem. Ref. Data* **38**, 33–94.

GUPTA, A. D. & STORVICK, T. S. 1970 Analysis of the heat conductivity data for polar and nonpolar gases using thermal transpiration measurements. *J. Chem. Phys.* **52** (2), 742–749.

HAAS, B. L., HASH, D. B., BIRD, G. A., LUMPKIN III, F. E. & HASSAN, H. A. 1994 Rates of thermal relaxation in direct simulation Monte Carlo methods. *Phys. Fluids* **6**, 2191.

HAEBEL, E. U. 1968 Measurement of the temperature dependence of the oscillation relaxation in sulphur hexafluoride between 10C and 215C. *Acustica* **20**, 65.

HANSON, F. B. & MORSE, T. F. 1967 Kinetic models for a gas with internal structure. *Phys. Fluids* **10**, 345.

JAEGER, F., MATAR, O. K. & MULLER, E. A. 2018 Bulk viscosity of molecular fluids. *J. Chem. Phys.* **148**, 174504.

LAMBERT, L. 1977 *Vibrational and Rotational Relaxation in Gases*. Clarendon.

LOYALKA, S. K. & STORVICK, T. S. 1979 Kinetic theory of thermal transpiration and mechanocaloric effect. III. Flow of a polyatomic gas between parallel plates. *J. Chem. Phys.* **71**, 339–350.

LOYALKA, S. K., STORVICK, T. S. & LO, S. S. 1982 Thermal transpiration and mechanocaloric effect. IV. Flow of a polyatomic gas in a cylindrical tube. *J. Chem. Phys.* **76** (8), 4157–4170.

MASON, E. A. 1963 Molecular relaxation times from thermal transpiration measurements. *J. Chem. Phys.* **39**, 522–526.

MASON, E. A. & MONCHICK, L. 1962 Heat conductivity of polyatomic and polar gases. *J. Chem. Phys.* **36**, 1622.

MAXWELL, J. C. 1867 On the dynamical theory of gases. *Phil. Trans. R. Soc.* **157**, 49–88.

MAXWELL, J. C. 1879 On stresses in rarefied gases arising from inequalities of temperature. Part 1. *Phil. Trans. R. Soc. Lond.* **170**, 231–256.

MEADOR, W. E., MINER, G. A. & TOWNSEND, L. W. 1996 Bulk viscosity as a relaxation parameter: fact or fiction? *Phys. Fluids* **8**, 258.

MEIJER, A. S., DE WIJN, A. S., PETERS, M. F. E., DAM, N. J. & VAN DE WATER, W. 2010 Coherent Rayleigh–Brillouin scattering measurements of bulk viscosity of polar and nonpolar gases, and kinetic theory. *J. Chem. Phys.* **133**, 164315.

PAN, X., SHNEIDER, M. N. & MILES, R. B. 2002 Coherent Rayleigh–Brillouin scattering. *Phys. Rev. Lett.* **89** (18), 183001.

PAN, X., SHNEIDER, M. N. & MILES, R. B. 2004 Coherent Rayleigh–Brillouin scattering in molecular gases. *Phys. Rev.* A **69**, 033814.

PAN, X., SHNEIDER, M. N. & MILES, R. B. 2005 Power spectrum of coherent Rayleigh–Brillouin scattering in carbon dioxide. *Phys. Rev.* A **71**, 045801.

PARKER, G. L. 1959 Rotational and vibrational relaxation in diatomic gases. *Phys. Fluids* **2**, 449–462.

PORODNOV, B. T., KULEV, A. N. & TUCHVETOV, F. T. 1978 Thermal transpiration in a circular capillary with a small temperature difference. *J. Fluid Mech.* **88** (4), 609–622.

QUINONES-CISNEROS, S. E., HUBER, M. L. & DEITERS, U. K. 2012 Correlation for the viscosity of sulfur hexafluoride (SF6) from the triple point to 1000 K and pressures to 50 MPa. *J. Phys. Chem. Ref. Data* **41**, 023102.

REYNOLDS, O. 1879 On certain dimensional properties of matter in the gaseous state. Part 1. *Phil. Trans. R. Soc. Lond.* **170**, 727–845.

SHANG, J. C., WU, T., WANG, H., YANG, C. Y., YE, C. W., HU, R. J., TAO, J. Z. & HE, X. D. 2019 Measurement of temperature-dependent bulk viscosities of nitrogen, oxygen and air from spontaneous Rayleigh–Brillouin scattering. *IEEE Access* **7**, 136439–136451.

SHARIPOV, F. 2011 Data on the velocity slip and temperature jump on a gas-solid interface. *J. Phys. Chem. Ref. Data* **40** (2), 023101.

SU, W., ZHU, L. H., WANG, P., ZHANG, Y. H. & WU, L. 2020 Can we find steady-state solutions to multiscale rarefied gas flows within dozens of iterations? *J. Comput. Phys.* **407**, 109245.

SUGAWARA, A., YIP, S. & SIROVICH, L. 1968 Spectrum of density fluctuations in gases. *Phys. Fluids* **11**, 925–932.

TENTI, G., BOLEY, C. & DESAI, R. 1974 On the kinetic model description of Rayleigh–Brillouin scattering from molecular gases. *Can. J. Phys.* **52**, 285.

VIEITEZ, M. O., VAN DUIJN, E. J., UBACHS, W., WITSCHAS, B., MEIJER, A., DE WIJN, A. S., DAM, N. J. & VAN DE WATER, W. 2010 Coherent and spontaneous Rayleigh–Brillouin scattering in atomic and molecular gases and gas mixtures. *Phys. Rev.* A **82**, 043836.

WAGNER, W. 1992 A convergence proof for Bird's direct simulation Monte Carlo method for the Boltzmann equation. *J. Stat. Phys.* **66**, 1011–1044.

WANG, Y., LIANG, K., VAN DE WATER, W., MARQUES, W. JR. & Ubachs, W. 2018 Rayleigh–Brillouin light scattering spectroscopy of nitrous oxide (N_2O). *J. Quant. Spectrosc. Radiat. Transfer* **206**, 63–69.

WANG, Y., UBACHS, W. & VAN DE WATER, W. 2019 Bulk viscosity of CO_2 from Rayleigh–Brillouin light scattering spectroscopy at 532 nm. *J. Chem. Phys.* **150**, 154502.

WANG, Y., YU, Y., LIANG, K., MARQUES, W. JR., van de Water, W. & Ubachs, W. 2017 Rayleigh–Brillouin scattering in SF_6 in the kinetic regime. *Chem. Phys. Lett.* **669**, 137–142.

WANG-CHANG, C. S. & UHLENBECK, G. E. 1951 Transport phenomena in polyatomic gases. Report No. CM-681. University of Michigan Engineering Research.

WHITE, F. M. 1998 *Viscous Fluid Flow*. McGraw-Hill Higher Education.

WU, L. & GU, X.-J. 2020 On the accuracy of macroscopic equations for linearized rarefied gas flows. *Adv. Aerodyn.* **2**, 2.

WU, L., LIU, H. H., ZHANG, Y. H. & REESE, J. M. 2015*a* Influence of intermolecular potentials on rarefied gas flows: fast spectral solutions of the Boltzmann equation. *Phys. Fluids* **27**, 082002.

WU, L. & STRUCHTRUP, H. 2017 Assessment and development of the gas kinetic boundary condition for the Boltzmann equation. *J. Fluid Mech.* **823**, 511–537.

WU, L., WHITE, C., SCANLON, T. J., REESE, J. M. & ZHANG, Y. H. 2015*b* A kinetic model of the Boltzmann equation for non-vibrating polyatomic gases. *J. Fluid Mech.* **763**, 24–50.